CME Geometry and the Production of Shocks and SEP Events

Stephen Kahler* **and Natchimuthuk Gopalswamy**†

**Air Force Research Laboratory/RVBXS, Hanscom AFB, MA 01731-3010*
†Laboratory for Solar Physics, NASA Goddard Space Flight Center, Greenbelt, MD 20771

Abstract**. Fast (V_{CME} $\geq$ 900 km/s) CMEs are usually associated with coronal shocks which are manifested by radio type II bursts in the metric through kilometric wavelength range. This association is expected when V_{CME} exceeds the characteristic Alfven speed in the corona, which ranges over ∼500-1500 km/s. However, some fast CMEs do not produce type II bursts and some type II bursts are associated with relatively slow (V_{CME} $<$ 700 km/s) CMEs. These results have been attributed to variations of the coronal V_A or to shocks unable to accelerate sufficient electrons to produce observable type II bursts. Recent heuristic arguments and modeling have made clear that the response of a magnetized plasma to the propagation of a CME depends on the CME geometry as well as its speed. A clear distinction is made between a projectile that propagates through the medium and can produce only a bow shock, and a 3-D piston that everywhere accretes material ahead of itself and may always produce a shock, given sufficient time and distance. The distinction between narrow projectile and broad piston CMEs offers an explanation for the observational result that essentially only CMEs with widths exceeding 60° are associated with either type II bursts or gradual solar energetic particle (SEP) events at 1 AU.**

Keywords**: Coronal mass ejections, shocks, solar energetic particles**

I. INTRODUCTION

The correlation of fast CME speeds with E $>$ 10 MeV SEP event peak intensities (Figure 1) has long been known [21]. The basic paradigm is that CMEs with $V_{CME} > V_A$, the plasma Alfven speed, drive shocks that accelerate seed particles to the high energies observed in space. Models of V_A versus coronal height generally place peak values at 3-10 R$_\circ$ and show $V_A < 500$ km/s above 10 R$_\circ$ [3]. Besides the CME speed requirement there is also an empirically observed requirement for a CME width $W_{CME} \geq 60°$ to produce gradual SEP events [13], [8]. Figure 2 shows that only the widest limb CMEs are associated with SEP events. While the intrinsic widths of the halo (W_{CME} = 360°) CMEs are not known and only lower limits to V_{CME} determined, it has been shown that halo CMEs must form a CME class both wider and faster than non-halo CMEs [16].

A similar minimum width requirement has been found [7], [8] for the production of interplanetary type II radio bursts in the decametric-hectometric (DH) range. The question now is why this requirement exists. One factor is the observed good correlation of ∼0.5-0.7 between V_{CME} and W_{CME} (Figure 2) [7], [6], although this does not explain the effective minimum requirement for W_{CME}. Here we discuss two fundamentally different ways shocks are produced by CME disturbances moving through plasmas that may explain better this W_{CME} dependence.

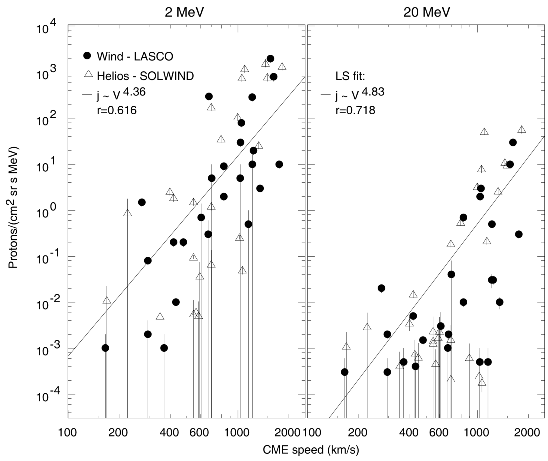

Fig. 1: The correlation of 2 and 20 MeV peak proton intensities versus V_{CME} for two different data sets, LASCO, •; Solwind, △. From [21]

II. TWO KINDS OF CME-DRIVEN SHOCKS

The shocks driven by interplanetary CMEs (ICMEs) moving through the solar wind have generally been modeled as bow shocks similar to, but weaker than, the Earth's bow shock [22], [23]. However, it has recently been appreciated that CME-driven shocks can be described by two fundamentally different processes [26], [31]. The first is the familiar bow shock, formed as solar wind flows around a relatively narrow projectile, and the second is an expansion shock, formed ahead of a piston driver expanding outward through the solar wind and accreting solar wind material ahead of itself. One difference is that the calculated shock standoff distance is smaller for the expansion shock than for the bow shock when normalized to the radius of the ICME [26]. Figure 3 compares the two shock standoff distances for a ratio of specific heats of γ = 5/3. Since the projectile ICME is assumed to have a fixed size, the standoff distance in a uniform medium is also fixed, but the shock standoff distance continually grows as the size of the

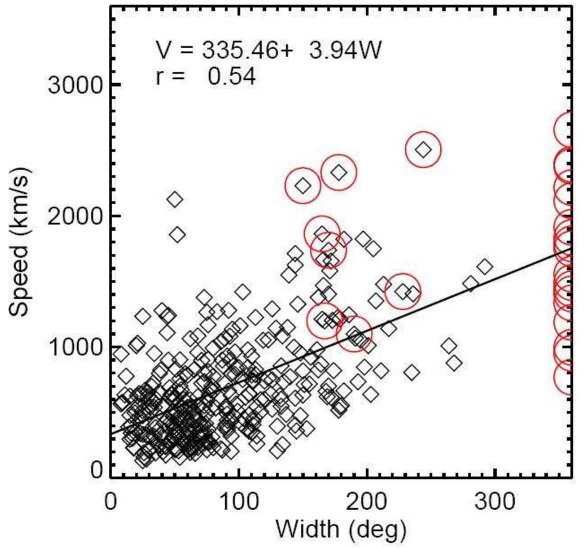

Fig. 2: Scatter plot showing the correlation between V_{CME} and W_{CME} for limb CMEs with solar source regions from W60° to the west limb. The CMEs with associated GOES SEP events are circled and the halo CMEs lie at W = 360°. From [6].

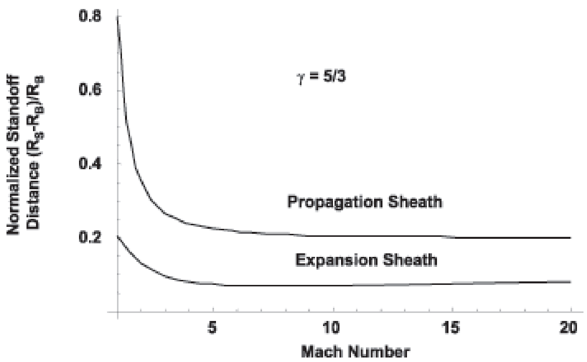

Fig. 3: Shock standoff distances normalized to the radius of the body as a function of Mach number. The curve labeled "Propagation Sheath" [22] is normalized to the radius of curvature at the nose. From [26].

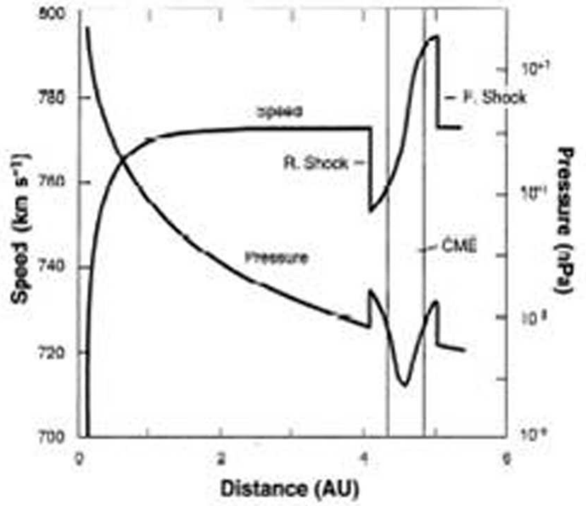

Fig. 4: Solar wind speed and pressure versus heliocentric distance for a simulated disturbance at 1 AU. The vertical lines identify the plasma of a density pulse introduced at 0.14 AU. The basic physics of the forward and reverse shocks are illustrated here with a 1-dimensional gasdynamic code. From [9].

expansion ICME increases by accreting solar wind. Note that in contrast to the Earth's bow shock, coronal and interplanetary shocks are characterized by the low Mach numbers [22] of the left side of Figure 3.

The ICME expansion shock was produced in a one-dimensional gasdynamic calculation [10] to model the high-latitude expansion ICMEs [9] discovered with the Ulysses spacecraft. Those ICMEs, described as "over-expanding" [9], were accompanied by forward-reverse shock pairs (Figure 4). Recent [34] more detailed calculations of ICME expansion shocks show that shock formation times and standoff distances are nearly independent of the plasma β, but are *shorter* for 1) higher CME speeds, 2) higher CME accelerations, and 3) larger Alfven Mach numbers and *longer* for 1) longer acceleration phase durations and 2) higher ambient V_A.

An important distinction between the two kinds of shocks is that $V_{CME} > V_A$ is required for the bow shock but not for the expansion shock. The latter can form even when V_{CME} is "subsonic" [34], [31]. However, those shocks can form only if the wave dissipation is sufficiently small [34], so we generally expect that most subsonic wide CMEs will not drive shocks. After launch the dynamics of the two ICME cases are also very different. The piston ICME can be described with the "snowplow" model [17], [27], and the projectile ICME by various drag models [30], [1], [32], although the magnetic reconnection of the projectile ICME fields with the ambient magnetic fields must be considered carefully [25] and stream structures can significantly distort the shape of the ICME magnetic flux rope [4]. CME or ICME-driven shocks are often combinations of the two kinds of shocks.

III. Expected consequences of CME-driven shocks

The distinction between the two kinds of CME-driven shocks has important consequences for the general association of gradual SEP events and fast CMEs. It suggests an explanation for the asymmetry of the SEP event associations of Figure 2, defined by an absence of SEP events for fast narrow CMEs and perhaps an enhancement of SEP events for slow broad CMEs.

A. Narrow fast projectile CMEs

We discussed the empirical ∼60° width requirement for both DH type II and SEP events in the introduction. In a recent study [18] of west limb CMEs with $V_{CME} >$ 900 km/s three radio-silent (lacking metric type II emission but not because of limb occultation) CMEs were

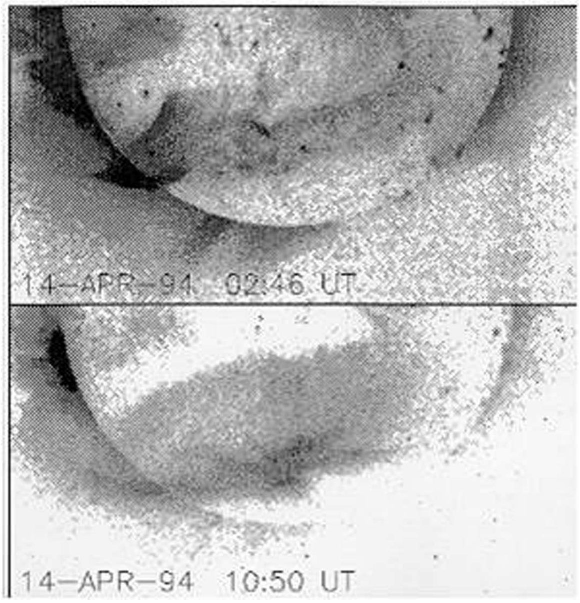

Fig. 5: Yohkoh soft X-ray negative images of the southern solar hemisphere associated with a large-scale filament eruption on 14 April 1994. The top image shows a cusp formation early in the event at the eastern end of an X-ray arcade spanning ~150° in longitude. The bottom image shows the westward extension of the arcade. This is one of three high-energy SEP events associated with eruptions outside solar active regions. From [14].

compared with a reference set of SEP-associated fast CMEs. The only significant difference was the narrower angular widths of the radio-silent CMEs, leading to the conclusion [18] that the SEP acceleration at shocks driven by narrow CMEs is either confined to small angular regions or less efficient than often thought. Our interpretation would be that the narrow CMEs act as projectiles to produce the narrower bow shocks rather the broader piston-driven shocks of wide CMEs. If shock acceleration occurs at the bow shocks, the narrower spatial acceleration region may produce either type II emission or SEP intensities too faint or weak to be observed at 1 AU. The reported widths of some CMEs may sometimes be overstated. An impressively fast and wide (V_{CME} = 2198 km/s, W_{CME} = 152°) CME on 7 April 2001 with no associated metric or DH type II burst had a bright core width of no more than ~80° [8]. The reported 152° width included possibly unrelated faint high-latitude spikey structures; the CME location behind the west limb may also have hindered observation of any type II burst.

If we suppose that there is a broad spectrum of fast CME widths, then the narrowest CMEs would produce nearly pure bow shocks and the broadest CMEs nearly pure piston shocks, with hybrid shock structures the more general result. Further assuming that both kinds of shocks can accelerate SEPs and ignoring distinctions between parallel and perpendicular shocks [28], [29], we can also ask about shock spectra from these shocks. The smaller size scales of the bow shocks may well lead to an absence of high-energy SEPs [33] compared with the spectra from the broader piston-driven shocks. This variation of effective cut-off energies with CME width is an effect that one can pursue observationally.

B. *Broad piston CMEs*

The fact that relatively slow piston CMEs can drive expansion shocks suggests that CMEs arising from eruptions of large filaments lying outside solar active regions (ARs) may be sources of SEP events. Energetic (E > 50 MeV) SEP events are nearly always associated with CMEs from flaring ARs, but at least three cases are known of energetic SEP events from eruptions of non-AR filaments. These unusual SEP events occurred in December 1971 [11], December 1981 [12], and April 1994 [14] (Figure 5). At lower (< 5 MeV) energies more such cases have been documented [24]. Slow piston CMEs near solar central meridian may be observed as halo CMEs associated with SEP events despite low V_{CME}. This may be the explanation of a pair of slow (V_{CME} < 500 km/s) halo CMEs associated with a SEP event on 30 October 2004 [20].

A piston CME may result from a driver with an extensive longitudinal range. This suggests that large eruptions from the solar back side may well drive shocks that extend over the solar limbs to produce SEP events at Earth. An E > 400 MeV SEP event observed on 16 August 2001 has been attributed to a halo CME originating at ~W180° [2]. Earlier prompt high energy SEP events from solar regions beyond ~W120° have also been reported [2].

Another manifestation of large longitudinal extents of piston CMEs may be their enhanced CME brightness. This was one interpretation of the result that among fast west-hemisphere CMEs the SEP-rich are bright but SEP-poor are faint [15]. CME masses increase statistically more than linearly with W_{CME}, as the log-log plot of Figure 6 shows for CMEs with $W_{CME} < 120°$ [5]. However, the average mass for well measured limb CMEs with associated metric and DH type II emission was $\sim 9.8 \times 10^{15}$g (arrow), more than the extrapolated value from the plot and more than an order of magnitude higher than that of the average CME. This in turn leads to an average kinetic energy of 1.8 $\times 10^{32}$ erg for those limb CMEs, more than two orders of magnitude higher than that of the average CME [5]. CME kinetic energies may prove to be an important organizing parameter in the association of type II bursts and SEP events with CMEs. A sample of large gradual SEP events has shown [19] that the ratio of SEP event energy to CME kinetic energy can average $\sim$ 10%.

IV. SUMMARY

The association of gradual SEP events with fast CMEs is well established. The paradigm is that CMEs drive fast-mode shocks at which SEPs are accelerated. It has

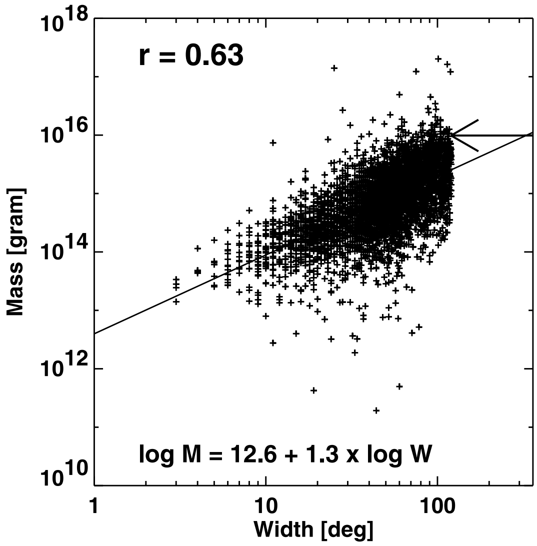

Fig. 6: Logarithmic scatter plot of CME mass versus W_{CME} for CMEs from 1996 to 2003 for which masses could be measured. Halo CMEs were omitted since their true widths can not be determined, but they are known to be faster and wider than those of the CME general population. The correlation coefficient r and regression line are indicated. The arrow marks the average mass of limb CMEs with type II burst associations. From [5].

not, however, been obvious why there are few if any gradual SEP events associated with narrow ($W_{CME} < 60°$) and fast CMEs. We suggest that the fundamental difference between the two extreme cases of projectile-driven bow shocks from the narrow CMEs and piston-driven shocks from the broad CMEs may account for this difference. SEP production in the CME bow shocks may be confined to relatively small spatial regions and/or only to lower energies. Complex CME fronts may produce shock structures involving both kinds of shocks that would undermine any simple relationship between CME width and peak SEP intensity. Several observational consequences for gradual SEP events may be accounted for within the context of our explanation.

V. Acknowledgements

N. Gopalswamy was supported by the NASA LWS TR&T program. S. Kahler was partially funded by AFOSR task 2301RDZ4. The LASCO CME data were taken from the CME catalog generated and maintained at the CDAW Data Center by NASA and The Catholic University of America in cooperation with the Naval Reserach Laboratory. SOHO is a project of international cooperation between ESA and NASA.

References

[1] P. J. Cargill (2004), Solar Phys., 221, 135.
[2] E. W. Cliver, B. J. Thompson et al. (2005), Proc. 29th ICRC, 1, 121.
[3] R. M. Evans, M. Opher, et al. (2008), Astrophys. J., 687, 1355.
[4] R. J. Forsyth, V. Bothmer et al. (2006), Space Sci. Rev., 123, 383.
[5] N. Gopalswamy, E. Aguilar-Rodriguez et al. (2005), J. Geophys. Res., 110, A12S07.
[6] N. Gopalswamy, A. Dal Lago et al. (2009), Cent. Eur. Astrophys. Bull., in press.
[7] N. Gopalswamy, N. Yashiro et al. (2001), J. Geophys. Res., 106, 29219.
[8] N. Gopalswamy, S. Yashiro et al. (2008), Ann. Geophys., 26, 3033.
[9] J. T. Gosling, D. J. McComas et al. (1994), Geophys. Res. Let., 21, 2271.
[10] J. T. Gosling, P. Riley et al. (1998), J. Geophys. Res., 103, 1941.
[11] S. W. Kahler (2001), Space Weather, AGU Geophys. Mon. 125, 109.
[12] S. W. Kahler, et al. (1986), Astrophys. J., 302, 504.
[13] S. W. Kahler and D. V. Reames (2003), Astrophys. J., 584, 1063.
[14] S. W. Kahler, H. V. Cane et al. (1998), J. Geophys. Res., 103, 12069.
[15] S. W. Kahler and A. Vourlidas (2005), J. Geophys. Res., 110, A12S01.
[16] A. Lara, N. Gopalswamy et al. (2006), J. Geophys. Res., 111, A06107.
[17] N. Lugaz, W. B. Manchester et al. (2005), Astrophys. J., 627, 1019.
[18] C. Marqué, A. Posner et al. (2006), Astrophys. J., 642, 1222.
[19] R. A. Mewaldt, C. M. S. Cohen, et al. (2005), Proc. 29th ICRC, 1, 129.
[20] S. Pohjolainen and N. J. Lehtinen (2006), A&A, 449, 359.
[21] D.V. Reames (2000), AIP Conf. Proc. 516, 26th ICRC, 289.
[22] C. T. Russell and T. Mulligan (2002), Planet. Space Sci., 50, 527.
[23] C. T. Russell and L. Jian (2007), Adv. Space Res., 41, 1177.
[24] B. Sanahuja, A. M. Heras et al. (1991), Solar Phys., 134, 379.
[25] J. M. Schmidt and P. J. Cargill (2003), J. Geophys. Res., 108, 1023.
[26] G. Siscoe and D. Odstrcil (2008), J. Geophys. Res., 113, A00B07.
[27] S. J. Tappin (2006), Solar Phys., 233, 233.
[28] A. J. Tylka, C. M. S. Cohen et al. (2005), Astrophys. J., 625, 474.
[29] A. J. Tylka and M. A. Lee (2006), Astrophys. J., 646, 1319.
[30] B. Vršnak and N. Gopalswamy (2002), J. Geophys. Res., 107, SSH 2.
[31] B. Vršnak and E.W. Cliver (2008), Sol. Phys., 253, 215.
[32] B. Vršnak, D. Vrbanec et al. (2008), A&A, 490, 811.
[33] G. P. Zank, W. K. M. Rice et al. (2000), J. Geophys. Res., 105, 25079.
[34] T. Žic, B. Vršnak, M. Temmer, and C. Jacobs (2008), Sol. Phys., 253, 237.